RECENT PROGRESS IN MATERIALS STUDIES WITH ACOUSTIC MICROSCOPY

R.C. Bray and C.F. Quate
Edward L. Ginzton Laboratory
Stanford University
Stanford, California 94305

ABSTRACT

The scanning acoustic microscope operating in water with a frequency of 2.5 GHz (wavelength 6000 Å) has been used to nondestructively characterize materials and devices in a manner inaccessible to optical and electron microscopy.

Adhesion of thin films of Cr on glass (optical masks for photolithography) is shown to be a strong source of acoustic microscope contrast. This offers nondestructive evaluation of film adhesion on a microscopic scale for the first time.

Study of intentionally damaged integrated circuit structures reveals damage features not visible in optical microscopy. Microscopic subsurface imaging of composite structures is presented, as in other recent acoustic microscope imaging of materials. Recent theoretical work in acoustic response of layered materials is reviewed.

The scanning reflection acoustic microscope reveals information complementary to that obtainable by optical and electron microscopy. The acoustic microscope is sensitive to the mechanical properties (stiffness, density, viscosity) of a sample. In some cases information unobtainable by any other nondestructive technique is revealed by acoustic microscopy.

In Fig. 1 a 10 nsec RF pulse applied to the ZnO transducer is converted into an acoustic plane wave pulse propagating in the sapphire towards the hemispherical lens. The lens focuses the sound wave to a diffraction limited spot in the water coupling the lens to the reflecting object, which is mechanically scanned in a raster pattern. The amplitude of the reflected acoustic pulse controls the brightness of a CRT display.

In Fig. 2, we see optical and acoustic micrographs of two samples of chromium on glass masks used for photolithography by a semiconductor manufacturer. In Figs. 2(a) – (c) the 1000 Å Cr film is well adhered to the glass substrate, as determined by the tape test and scratch test for film adhesion. The contrast is uniform across the Cr area of all three pictures. In the acoustic micrographs this indicates uniformity of mechanical properties.

In Figs. 2(d) – (f), micrographs of poorly adhering Cr, the contrast around the edges of the Cr regions indicates different adhesion from the central, presumably better adhered areas. In the optical photo the only evidence of poor adhesion is nicks where the Cr has actually peeled off. The acoustic image can thus show areas of poor film adhesion nondestructively.

In Fig. 3 we see acoustic micrographs at different focal positions of an aluminum line on silicon. The quartz passivation layer on top has been purposely damaged with a diamond indenter. The radial pattern of lines diverging away from the damaged area are mostly not visible in the optical oil immersion micrograph. We believe these are microcracks in the quartz passivation layer and in the silicon substrate. The width of the Aℓ line is 15 μ and the width of the cracks is near the 5000 Å resolution limit of the acoustic microscope at 2.6 GHz.

Figure 4 shows optical and acoustic images of a composite material fabricated by Dupont; hollow glass spheres imbedded in polyethylene. There are several spheres visible in the acoustic images which are completely absent from the optical picture. They are below the surface of the optically opaque polyethylene matrix. Because of the good impedance match between water ($Z = 1.55$ and 10^5 gm/cm^2 sec) polyethyelene ($Z = 1.7 \times 10^5$ gm/cm^2 sec), the polyethylene is transparent to sound and subsurface spheres are easily imaged.

Figures 5 and 6 show polished materials samples in which features are visible in the acoustic micrographs of the polished but unetched samples which are completely invisible in the optical micrographs of the matched sample. Grain boundaries and twin lines visible in acoustic micrographs of the unetched Si sample in Fig. 5 become visible optically only when the sample is etched.

In the case of the polished inconel (Ni/Cr/Fe alloy) sample, there are in fact twin lines within individual grains which are visible in the acoustic images but are not visible even in the optical micrograph of the etched sample. This alloy has similar etch rates for different crystal orientations, so optical images of etched samples mainly reveal the grain boundaries, where the etch rate is higher. The acoustic images reveal a high degree of contrast between different grains, and even within what etching would appear to define as individual grains. We attribute this to the anisotropy of the crystallites and the resultant difference in acoustic reflectance.

We have written the necessary programs to calculate predicted acoustic microscope response for samples consisting of plane solid layers on a solid substrate. The microscope detected power output is plotted versus lens-object spacing Z, as in Fig. 7. In this graph, the curves represent the predicted

microscope $V(Z)$ for three different samples: Glass, 1000 Å Cr well adhered to glass, and 1000 Å of Cr with a vacuum layer between it and glass. The predicted relative contrasts between three such areas in a single acoustic microscope image can be found by noting the three values of $V(Z)$ for a fixed lens - object spacing Z.

The important point about the $V(Z)$ plots at hand is that they successfully predict observed contrast in the acoustic micrographs of well adhered and poorly adhered chromium on glass. They also show that poor adhesion is expected to be directly observable in acoustic micrographs, as we observe from Fig. 2 to be the case. We choose to model a poorly adhering Cr film as a thin layer of vacuum between film and substrate.

In summary we have presented examples of the acoustic microscope's ability to reveal information about materials and structures which is not readily obtainable by any other nondestructive technique.

This work was supported by the Air Force Office of Scientific Research under Contract F49620-78-C-0098.

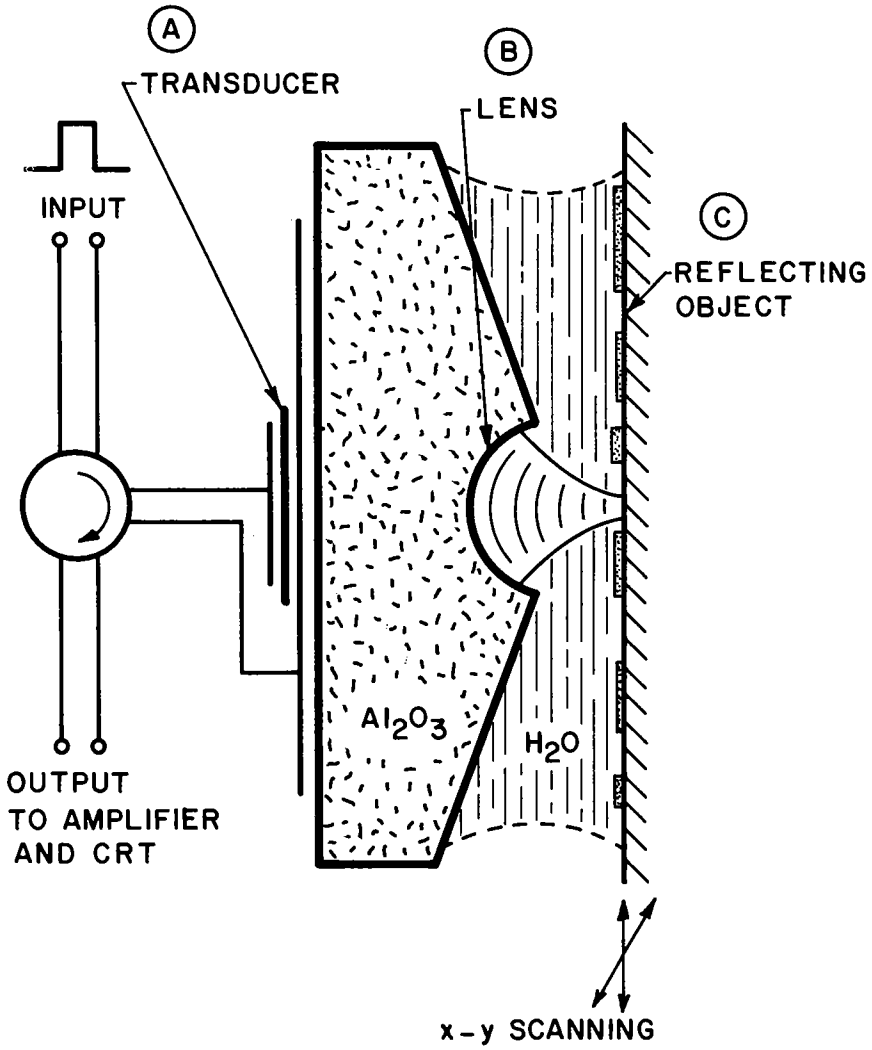

FIG. 1--Acoustic lens.

1000 A Cr ON GLASS (GOOD ADHESION)

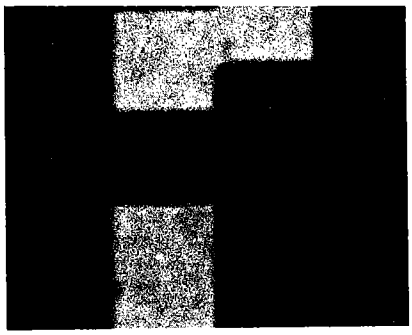

30 μ

(a) OPTICAL

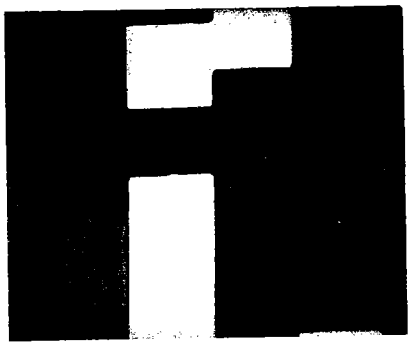

(b) ACOUSTIC, FOCUSED ON Cr

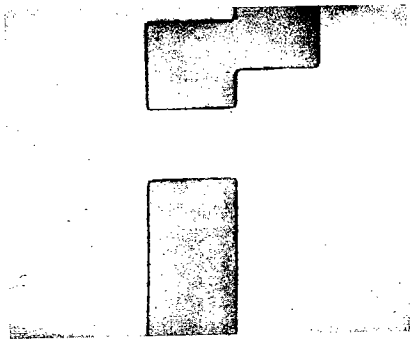

(c) ACOUSTIC, FOCUSED ON GLASS

1000 A Cr ON GLASS (POOR ADHESION)

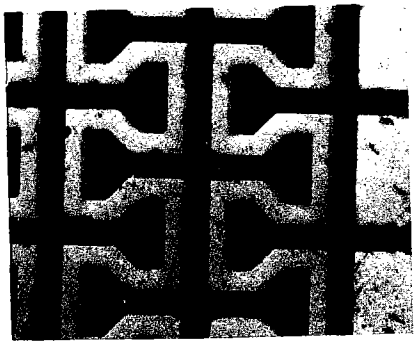

100 μ

(d) OPTICAL

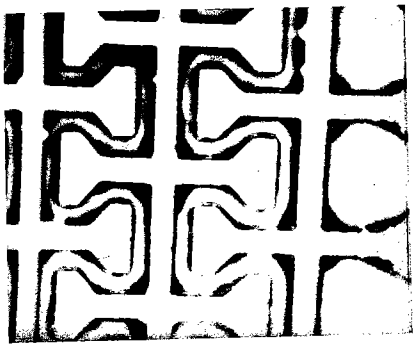

(e) ACOUSTIC $Z = -1\mu$

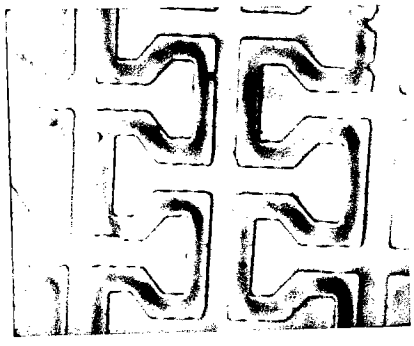

(f) ACOUSTIC $Z = -0.5\mu$

FIGURE 2

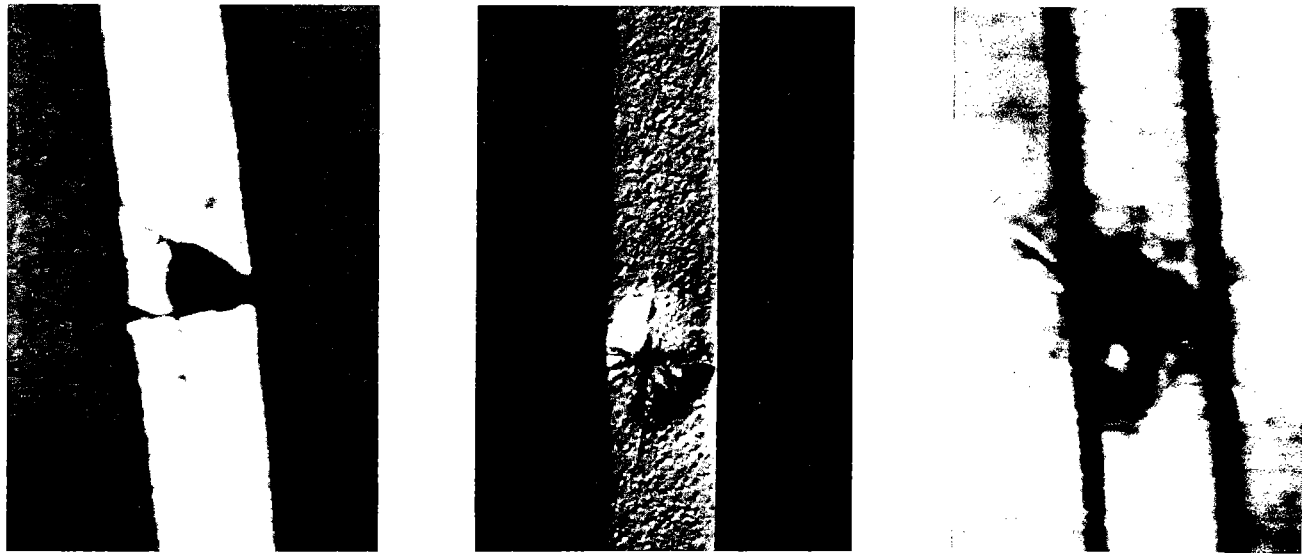

(a) ACOUSTIC 1st FOCUS

(b) OPTICAL

(c) ACOUSTIC 2nd FOCUS

ALUMINUM LINE ON SILICON WITH QUARTZ OVERLAY

FIGURE 3

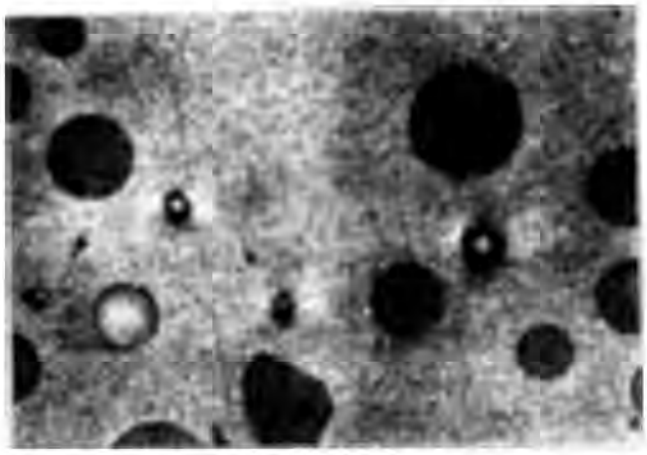

(a) OPTICAL x620

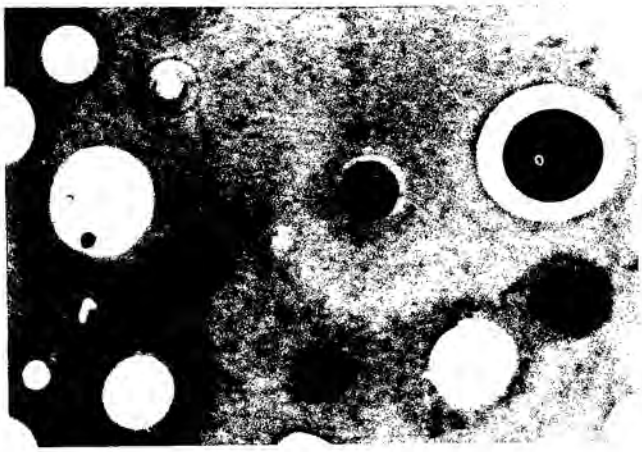

(b) ACOUSTIC (2600 MHz)

POLYETHYLENE TEREPHTHALATE
WITH IMBEDDED GLASS BEADS

FIGURE 4

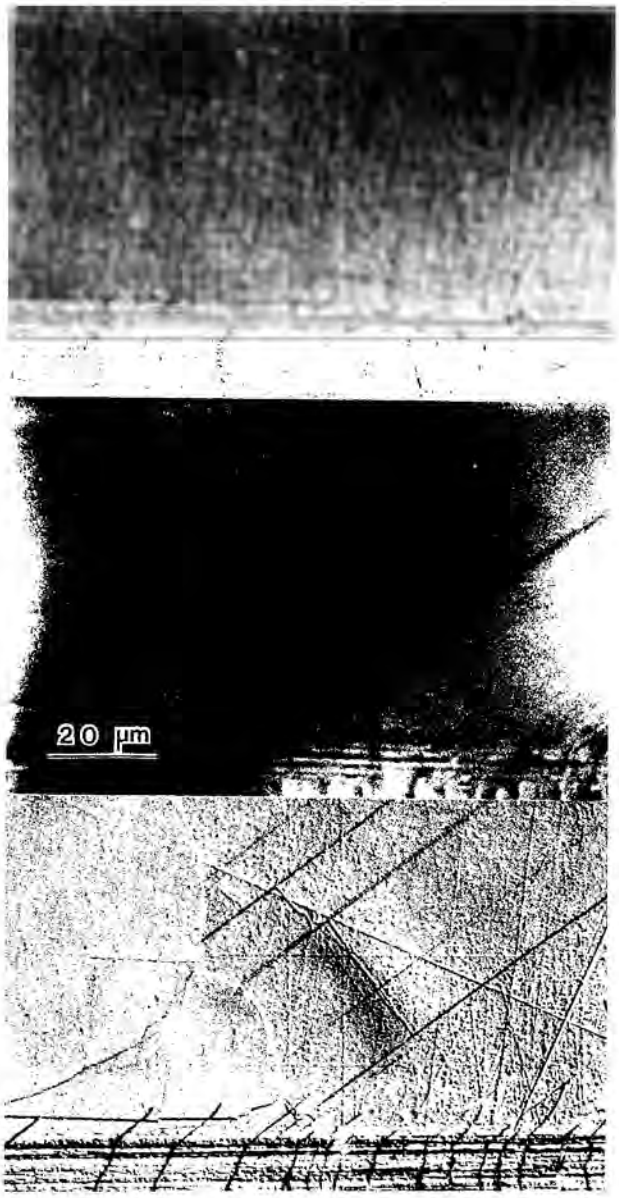

FIG. 5--(Top) Optical micrograph of polished Si sample.
(Center) Acoustic micrograph of same area f = 2.5 GHz.
(Bottom) Optical micrograph of same area after etching.

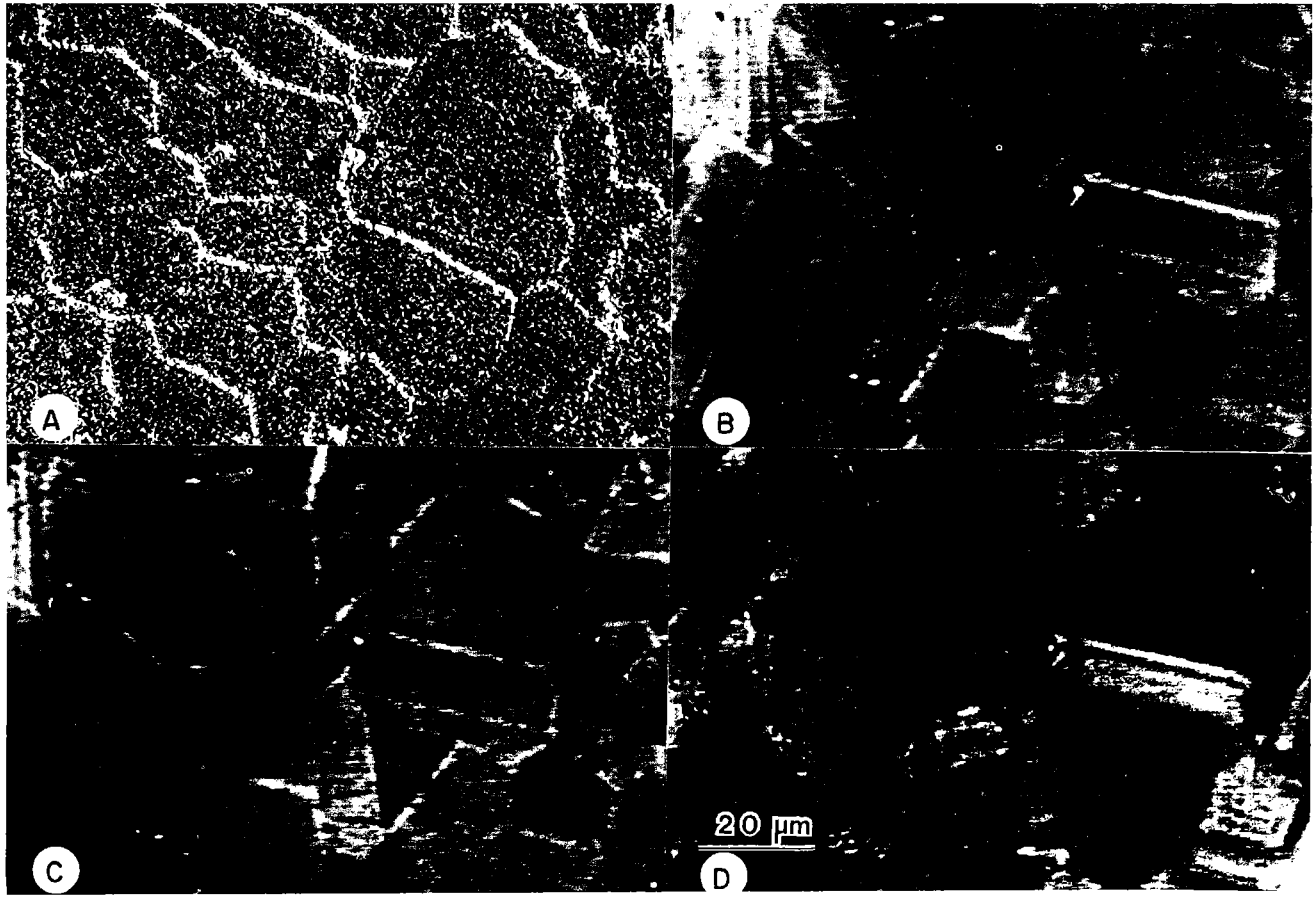

FIG. 6--Inconel alloy. (A) Optical micrograph after etching; (B), (C), (D) 2.5 GHz acoustic micrographs of unetched sample at three different focal positions ($z = -1\mu, -2\mu, -4\mu$).

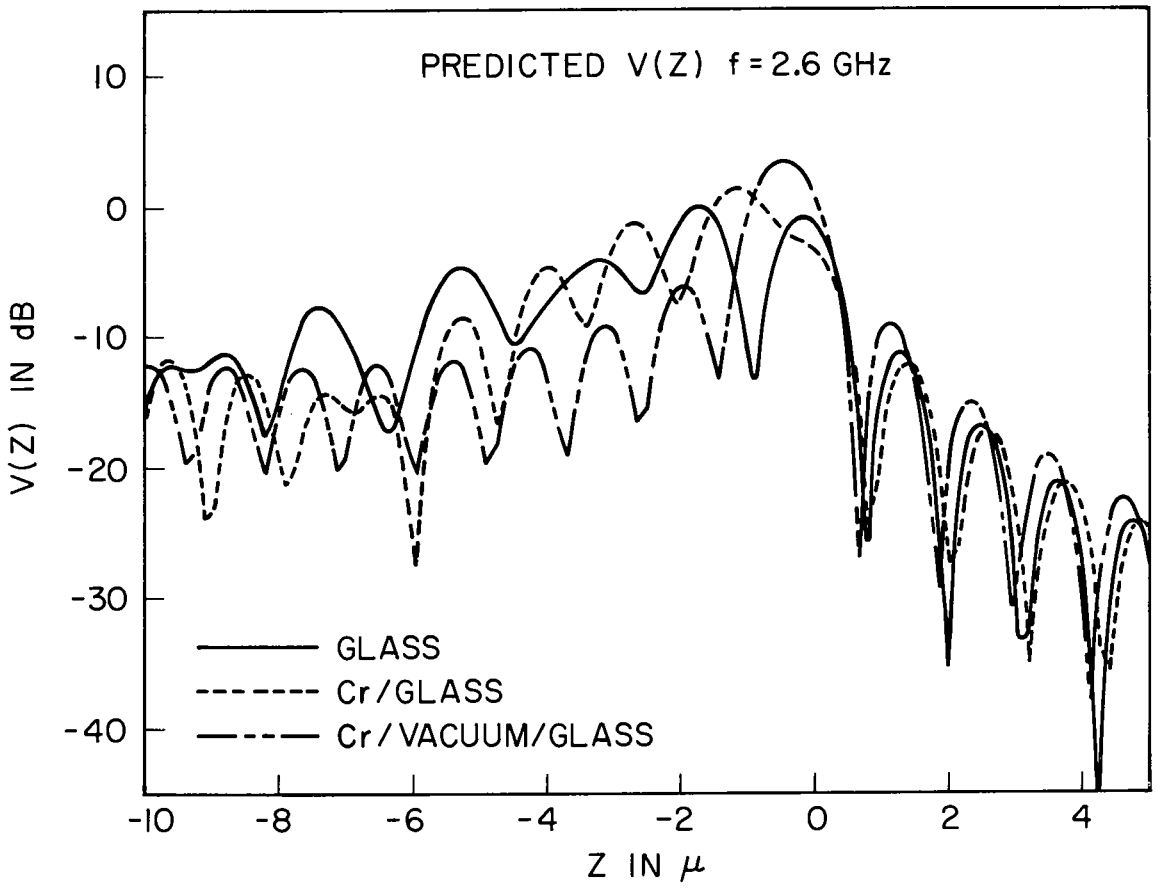
PREDICTED V(Z) f = 2.6 GHz
10
0
-10
-20
-30
-40
V(Z) IN dB
GLASS
Cr/GLASS
Cr/VACUUM/GLASS
-10
-8
-6
-4
-2
0
2
4
Z IN μ

FIGURE 7